

ORIGINAL RESEARCH

Association Between Left Ventricular Mechanical Deformation and Myocardial Fibrosis in Nonischemic Cardiomyopathy

Ibolya Csecs , MD; Farhad Pashakhanloo, PhD; Amanda Paskavitz, BA; Jihye Jang, PhD; Talal Al-Otaibi, MD; Ulf Neisius, MD, PhD; Warren J. Manning, MD; Reza Nezafat , PhD

BACKGROUND: In patients with nonischemic cardiomyopathy, nonischemic fibrosis detected by late gadolinium enhancement (LGE) cardiovascular magnetic resonance is related to adverse cardiovascular outcomes. However, its relationship with left ventricular (LV) mechanical deformation parameters remains unclear. We sought to investigate the association between LV mechanics and the presence, location, and extent of fibrosis in patients with nonischemic cardiomyopathy.

METHODS AND RESULTS: We retrospectively identified 239 patients with nonischemic cardiomyopathy (67% male; 55±14 years) referred for a clinical cardiovascular magnetic resonance. LGE was present in 109 patients (46%), most commonly (n=52; 22%) in the septum. LV deformation parameters did not differentiate between LGE-positive and LGE-negative groups. Global longitudinal, radial, and circumferential strains, twist and torsion showed no association with extent of fibrosis. Patients with septal fibrosis had a more depressed LV ejection fraction (30±12% versus 35±14%; $P=0.032$) and more impaired global circumferential strain ($-7.9\pm3.5\%$ versus $-9.7\pm4.4\%$; $P=0.045$) and global radial strain (10.7±5.2% versus 13.3±7.7%; $P=0.023$) than patients without septal LGE. Global longitudinal strain was similar in both groups. While patients with septal-only LGE (n=28) and free wall-only LGE (n=32) had similar fibrosis burden, the septal-only LGE group had more impaired LV ejection fraction and global circumferential, longitudinal, and radial strains (all $P<0.05$).

CONCLUSIONS: There is no association between LV mechanical deformation parameters and presence or extent of fibrosis in patients with nonischemic cardiomyopathy. Septal LGE was associated with poor global LV function, more impaired global circumferential and radial strains, and more impaired global strain rates.

Key Words: cardiac magnetic resonance imaging ■ late gadolinium enhancement ■ myocardial mechanics ■ nonischemic dilated cardiomyopathy ■ strains

Cardiovascular magnetic resonance (CMR) is the noninvasive gold standard for assessment of left ventricular (LV) function and tissue characterization by late gadolinium enhancement (LGE) in patients with nonischemic cardiomyopathy (NICM).^{1,2} In NICM, presence of LV fibrosis detected by LGE is associated with adverse cardiovascular outcomes.^{3,4} LGE is present in 30% to 40% of patients with NICM in the midmyocardial septum.^{3,4} However, the characteristics of focal fibrosis in NICM are variable and can involve

other locations such as the LV free wall.^{3,4} Differences in fibrosis pattern, extent, and location in NICM may have diverse effects on LV function and mechanics. Assessment of myocardial deformation by CMR feature tracking could provide additional diagnostic and prognostic information in patients with impaired LV function, incremental to the principal measure of LV ejection fraction (LVEF).^{5,6}

Previous CMR tissue tracking studies reported depressed longitudinal and circumferential shortening in

Correspondence to: Reza Nezafat, PhD, Cardiovascular Division, Department of Medicine, Beth Israel Deaconess Medical Center and Harvard Medical School, 330 Brookline Avenue, Boston, MA 02215. E-mail: rnezafat@bidmc.harvard.edu

Supplementary Materials for this article are available at <https://www.ahajournals.org/doi/suppl/10.1161/JAHA.120.016797>

For Sources of Funding and Disclosures, see page 10.

© 2020 The Authors. Published on behalf of the American Heart Association, Inc., by Wiley. This is an open access article under the terms of the Creative Commons Attribution-NonCommercial-NoDerivs License, which permits use and distribution in any medium, provided the original work is properly cited, the use is non-commercial and no modifications or adaptations are made.

JAHA is available at: www.ahajournals.org/journal/jaha

CLINICAL PERSPECTIVE

What Is New?

- In patients with nonischemic cardiomyopathy, no association was found between left ventricular (LV) mechanical deformation parameters and presence or extent of fibrosis; however, the location of late gadolinium enhancement was an important determinant of LV mechanics: Septal late gadolinium enhancement was associated with poor global LV function, more impaired global circumferential strain and global radial strain compared with patients without late gadolinium enhancement.
- Our study is the first to investigate the relation between the presence of left bundle branch block and LV torsional parameters using cardiac magnetic resonance feature tracking in a large group of patients with nonischemic cardiomyopathy.
- We found that left bundle branch block and consequential cardiac dyssynchrony is associated with reverse basal circumferential rotation and reduction of LV twist and torsion.

What Are the Clinical Implications?

- We described the association of nonischemic fibrosis located in the LV septum and impaired LV function and mechanics.
- In the future, our results might have an importance in clinical prognostication of patients with nonischemic cardiomyopathy and could help to develop individual targeted therapy.

Nonstandard Abbreviations and Acronyms

| | |
|-------------|-------------------------------|
| DSR | diastolic strain rate |
| GCS | global circumferential strain |
| GLS | global longitudinal strain |
| GRS | global radial strain |
| LGE | late gadolinium enhancement |
| NICM | nonischemic cardiomyopathy |
| SSR | systolic strain rate |

patients with NICM.⁷⁻¹⁰ LV torsion, which is the relative rotation of the LV apex to the base generated by circumferentially oriented midmyocardial fibers, was also found to be impaired in this group.^{8,11} Currently, there are no available data demonstrating how the different locations of focal nonischemic fibrosis impact LV torsion in patients with NICM.

In patients with ischemic cardiomyopathy, sub-endocardial-transmural scars in the coronary artery

distribution are associated with impaired global and regional strains.¹²⁻¹⁴ In patients with hypertrophic cardiomyopathy, global longitudinal strain (GLS) correlates with the extent of LGE (expressed as a percentage of LV mass) in the overall cohort, but not in the LGE-positive group separately.^{15,16} In NICM, areas of LGE are most commonly located in the midmyocardium. The impact of LGE location and extent on the mechanical parameters in NICM, however, is not fully known. In this study, we sought to investigate the association between LGE and LV mechanical deformation parameters using CMR feature tracking.

METHODS

Study Population

The study was Health Insurance Portability and Accountability Act compliant and approved by the Beth Israel Deaconess Medical Center Institutional Review Board. Written informed consent was obtained from each participant for use of their CMR images for research. We retrospectively identified patients with NICM referred for a clinical CMR at our center between May 2012 and May 2019. The diagnosis of NICM was confirmed using information extracted from electronic medical records. We excluded patients with (1) hypertrophic, inflammatory, infiltrative, and arrhythmogenic cardiomyopathies; (2) ischemic coronary disease defined as a history of myocardial infarction, presence of epicardial coronary artery diameter stenosis >70%, or presence of a subendocardial/transmural pattern of LGE; (3) documented genetic arrhythmias (eg, Brugada, long QT syndrome); and (4) impaired renal function as contraindication of contrast administration. All clinical information and diagnoses were reviewed case by case using online medical records. The data that support the findings of this study are available from the corresponding author upon reasonable request.

CMR Image Acquisition

CMR imaging was performed on a 1.5 T CMR system (Achieva, Philips Healthcare, Best, The Netherlands) equipped with a 32-channel cardiac coil or a 3 T CMR system (Vida, Siemens Healthineer, Erlangen, Germany) using an 18-channel body coil. Breath-hold, retrospectively gated cine images were collected using the balanced steady-state free-precession sequence in the 2- and 4-chamber long-axis LV views in the LV outflow tract view and short-axis stack covering the entire LV (8-mm slices with 2-mm gaps). LGE images were obtained using a 3-dimensional phase-sensitive inversion-recovery sequence with a spectral fat saturation prepulse during the end-diastolic phase ≈ 15 minutes after administration (gadobenate dimeglumine 0.1 mmol/kg, Multihance, Bracco Diagnostics Inc.,

Monroe Township, NJ; or 0.2 mmol/kg gadopentetate dimeglumine Magnevist, Bayer Schering Pharma AG, Berlin, Germany).

CMR Image Analysis

LV Deformation Analysis by Tissue Tracking

LV deformation analysis was performed using CVI42 (v. 5.10.1, Circle Cardiovascular Imaging Inc. Calgary, Canada).^{16–18} LV endo- and epicardial borders were manually traced at end diastole in ECG-gated balanced steady-state free precession short- and long-axis (2- and 4-chamber, LV outflow tract) sequences. Automatic border tracking was applied to track image features throughout the cardiac cycle. Tracking was visually reviewed and manually corrected. Global circumferential (GCS), longitudinal (GLS), and radial (GRS) strains were assessed. Corresponding systolic (SSR) (SSR_C, SSR_L, SSR_R) and diastolic strain rates (DSR) (DSR_C, DSR_L, DSR_R) were also evaluated, representing the velocity of the deformation during systole and diastole. Global circumferential and radial strain values were calculated as the average of the mean curves of all LV segments on the short-axis stack, and longitudinal strain values as the average of the mean curves of the long-axis slices (2- and 4-chamber, LV outflow tract). The basal and apical circumferential peak systolic rotations were measured on short-axis cines. As viewed from the apex, the basal rotation is clockwise and expressed as a negative value, while apical rotation is counterclockwise and expressed as a positive value. Systolic rotation was expressed as a net maximum extent of rotation in the anticipated direction (eg, clockwise [+]) basal rotation was calculated as zero value) and as a magnitude of rotation regardless of the direction of movement. LV twist was defined as the net difference between the apical and basal rotation; twist per unit length was calculated by dividing LV twist by base-to-apex length of the LV.¹⁹ LV torsion, representing the rotation of the apex relative to the base, was calculated as follows:

$$((\Theta_{\text{apical}} \times r_{\text{apical}}) - (\Theta_{\text{basal}} \times r_{\text{basal}})) / D$$

where Θ , r , and D represent rotation, radius, and base-to-apex length, respectively.^{19–21} Inter- and intraobserver variability of LV mechanical parameters was tested on 40 randomly selected scans. To enable calculating the strain, a minimum of 25 cardiac phases were required in cine images; therefore, we had to exclude patients who had fewer than 25 time frames in the standard cine images.

LGE Analysis

LGE presence, extent (g), and LGE% (ie LGE [g]/LV mass [g]×100) were assessed by a reader with

5 years of CMR imaging experience using a 5 SD threshold. This threshold was chosen based on prior studies involving identification of LGE in patients with NICM.^{22–24} The scar location of LGE was assessed using the 17-segment American Heart Association model.

Statistical Analysis

Statistical analyses were performed using MedCalc 13.2.2 (MedCalc Software, Ostend, Belgium). The Kolmogorov–Smirnov test was used to assess the normal distribution of the data. Continuous variables were reported as mean±SD or median with an interquartile range (IQR) for normally distributed and skewed continuous variables, respectively. Categorical and ordinal variables were reported as frequencies or percentage. Comparisons between groups were made using the Student t test, Wilcoxon rank sum test, or Fisher's exact test. The associations between variables were assessed using linear or logistic regression. Interobserver agreement was evaluated with an intraclass correlation coefficient.²⁵ A P value of <0.05 was considered to be significant.

RESULTS

Study Population

The final cohort comprised 239 patients (67% male; mean age, 55±14 years). Ninety-two patients (39%) had hypertension, 51 patients (21%) had diabetes mellitus, and 55 patients (23%) had hyperlipidemia. Forty patients (17%) had a history of at least 1 nonsustained/sustained ventricular tachycardia or ventricular fibrillation episode before the CMR scan, while 25 patients (11%) had documented atrial fibrillation or atrial flutter. Fifty-six (23%) patients had left bundle branch block (LBBB) at the time of the CMR scan. Patients who were LGE negative had LBBB more often than patients who were LGE positive (31% versus 15%; $P=0.038$) (Table 1).

Presence of Focal Fibrosis

LGE was present in 109 patients (46%). The mean age, sex, and body surface area were similar among LGE-negative and LGE-positive groups (Table 1). Patient comorbidities such as hypertension, diabetes mellitus, and hyperlipidemia were similar between LGE-positive and LGE-negative groups. Twenty-two patients (17%) in the LGE-negative group and 18 patients (17%) in the LGE-positive group had a history of documented ventricular tachycardia/ventricular fibrillation. LV and right ventricular (RV) end-diastolic volume, mass, and mass index were higher in the LGE-positive group, although LVEF was similar (Table 1). Regarding LV mechanics, none of

Table 1. Patients' Characteristics and Cardiac Magnetic Resonance Parameters in Non-Ischemic Cardiomyopathy Patients

| Variables | Total N=239 | LGE Positive N=109 | LGE Negative N=130 | P Value (LGE Positive vs LGE Negative) |
|---------------------------|----------------|-----------------------|-----------------------|---|
| Age, y | 55±14 | 55±14 | 54±14 | 0.855 |
| Male, n (%) | 159 (67) | 74 (68) | 85 (65) | 0.683 |
| BSA, m ² | 2.00±0.3 | 2.10±0.26 | 2.00±0.28 | 0.423 |
| Clinical history | | | | |
| Heart rate, beat/min | 76±17 | 76±17 | 75±17 | 0.453 |
| Hypertension, n (%) | 92 (39) | 48 (44) | 44 (34) | 0.108 |
| Diabetes mellitus, n (%) | 51 (21) | 18 (17) | 33 (25) | 0.096 |
| Hyperlipidemia, n (%) | 55 (23) | 23 (21) | 32 (24) | 0.521 |
| VT/VF, n (%) | 40 (17) | 18 (17) | 22 (17) | 0.933 |
| LBBB, n (%) | 56 (23) | 16 (15) | 40 (31) | 0.038* |
| AF/AFL, n (%) | 25 (11) | 12 (11) | 14 (11) | 0.953 |
| Left ventricle | | | | |
| LVEDV, mL | 268±85 | 282±93 | 257±76 | 0.022* |
| LVEDVi, mL/m ² | 131±36 | 137±39 | 128±32 | 0.040* |
| LVESV, mL | 184±89 | 197±100 | 174±78 | 0.049* |
| LVESVi, mL/m ² | 90±40 | 95±44 | 86±34 | 0.084 |
| LVSV, mL | 83±26 | 84±26 | 81±26 | 0.471 |
| LVSVi, mL/m ² | 41±12 | 41±13 | 41±12 | 0.758 |
| LVEF, % | 34±14 | 33±14 | 34±13 | 0.535 |
| LVM, g | 146±49 | 154±47 | 140±49 | 0.017* |
| LVMi, g/m ² | 72±20 | 75±19 | 69±21 | 0.045* |
| Right ventricle | | | | |
| RVEDV, mL | 184±60 | 193±64 | 177±55 | 0.036* |
| RVEDVi, mL/m ² | 91±25 | 94±26 | 88±24 | 0.105 |
| RVESV, mL | 105±56 | 106±61 | 105±52 | 0.914 |
| RVESVi, mL/m ² | 51±25 | 55±27 | 48±23 | 0.029* |
| RVSV, mL | 79±25 | 80±24 | 79±26 | 0.651 |
| RVSVi, mL/m ² | 39±12 | 39±11 | 39±12 | 0.976 |
| RVEF, % | 46±14 | 44±15 | 47±13 | 0.113 |
| RVEDV/LVEDV | 0.71±0.2 | 0.71±0.19 | 0.71±0.20 | 0.990 |
| Left ventricular fibrosis | | | | |
| LGE, g | | 5.0 [3.8–6.3] | ... | ... |
| LGE% | | 3.4 [2.8–4.4] | ... | ... |

AF indicates atrial fibrillation; AFL, atrial flutter; BSA, body surface area; LGE, late gadolinium enhancement; LVEDV, left ventricular end-diastolic volume; LVEDVi, left ventricular end-diastolic volume index; LVEF, left ventricular ejection fraction; LVESV, left ventricular end-systolic volume; LVESVi, left ventricular end-systolic volume index; LVM, left ventricular mass; LVMi, left ventricular mass index; LVSV, left ventricular stroke volume index; LVSVi, left ventricular stroke volume index; RVEDV, right ventricular end-diastolic volume; RVEDVi, right ventricular end-diastolic volume index; RVEF, right ventricular ejection fraction; RVESV, right ventricular end-systolic volume; RVESVi, right ventricular end-systolic volume index; RVSV, right ventricular stroke volume; RVSVi, right ventricular stroke volume index; VF, ventricular fibrillation; and VT, ventricular tachycardia.

*Significant value ($P < 0.05$).

the investigated mechanical parameters discriminated between the LGE-positive and LGE-negative cohorts (Table 2). GLS, GCS, and GRS correlated with LVEF in the whole cohort and in the LGE-negative and LGE-positive groups separately (Figure 1A). The corresponding SSRs (SSR_C , SSR_L , SSR_R) and DSRs (DSR_C , DSR_L , DSR_R) also correlated with LVEF (all $P < 0.05$). The presence of LGE did not correlate significantly with LV mechanical parameters

(GLS, GCS, GRS) or strain rates (SSR_C , SSR_L , SSR_R , DSR_C , DSR_L , DSR_R) in the whole cohort (correlation coefficients $|r| < 2$ and P values are not significant). Similarly, torsion and twist did not correlate with presence of LGE.

Extent of Focal Fibrosis

In the LGE-positive group, the median amount of the fibrosis was 5.0 g (IQR, 3.8–6.3) and LGE% was 3.4%

Table 2. Left Ventricular Mechanical Parameters in Patients With and Without Fibrosis

| Variables | LGE Positive (N=109) | LGE Negative (N=130) | P Value |
|-----------------------------|----------------------|----------------------|---------|
| GCS, % | -9.2±4.4 | -9.0±4.1 | 0.804 |
| SSR _C (1/s) | -0.50±0.23 | -0.52±0.24 | 0.532 |
| DSR _C (1/s) | 0.47±0.22 | 0.53±0.28 | 0.058 |
| GLS, % | -8.7±4.1 | -8.6±4.0 | 0.731 |
| SSR _L (1/s) | -0.46±0.19 | -0.50±0.20 | 0.999 |
| DSR _L (1/s) | -0.46±0.19 | -0.49±0.19 | 0.112 |
| GRS, % | 13.0±8.0 | 12.4±7.3 | 0.606 |
| SSR _R (1/s) | 0.68±0.35 | 0.67±0.38 | 0.952 |
| DSR _R (1/s) | -0.65±0.39 | -0.65±0.50 | 0.932 |
| Basal systolic rotation, ° | | | |
| Net clockwise | -1.4±1.0 | -1.6±1.2 | 0.161 |
| Magnitude | -1.2±1.5 | -1.4±1.5 | 0.170 |
| Apical systolic rotation, ° | | | |
| Net counterclockwise | 1.6±2.9 | 1.2±2.7 | 0.074 |
| Magnitude | 1.7±3.0 | 1.2±2.9 | 0.249 |
| Twist, ° | 2.9±2.8 | 2.8±2.4 | 0.607 |
| Twist per length, °/cm | 0.44±0.4 | 0.41±0.4 | 0.649 |
| Torsion, °s ⁻¹ | 1.43±1.1 | 1.31±0.9 | 0.374 |

DSR_C indicates circumferential diastolic strain rate; DSR_L, longitudinal diastolic strain rate; DSR_R, radial diastolic strain rate; GCS, global circumferential strain; GLS, global longitudinal strain; GRS, global radial strain; LGE, late gadolinium enhancement; SSR_C, circumferential systolic strain rate; SSR_L, longitudinal systolic strain rate; and SSR_R, radial systolic strain rate.

*Significant value ($P < 0.05$).

(IQR, 2.8–4.4). There was no correlation between the extent of fibrosis and ejection fraction, volumes and mass indexes, or any LV mechanical parameters (GCS, GLS, GRS, SSR_C, SSR_L, SSR_R, DSR_C, DSR_L, DSR_R, twist, twist per length and torsion). To further analyze the impact of LGE extent on LV mechanical parameters, we divided the LGE-positive cohort into subgroups with LGE% <3.41% (n=54) and LGE% >3.41% (n=55). Patients with greater LGE% had higher LV mass (LV mass index, 79±19 g/m² versus 71±19 g/m²; $P=0.026$), but no difference was found regarding LV function or mechanical parameters. To further stratify patients with LGE, we compared patients who were LGE positive with LVEF >35% (n=43) and severely impaired LV function (LVEF <35% n=66) and found that LGE% did not correlate with global strain values (Figure 1B).

Location of Focal Fibrosis

Midmyocardial fibrosis was present in 74 patients (31% of whole cohort), while subepicardial LGE in a noncoronary distribution was present in 21 patients (9%). LGE mainly involved the basal segments

(36%), specifically the basal antero- and inferoseptal segments, followed by the basal and midinferolateral segments (Figure 2). Twenty-three (10%) patients had LGE limited to the RV anterior or inferior insertion zones. Comparisons between patients with (n=52) and without midmyocardial septal fibrosis (n=187) showed that the septal LGE group had a decreased LVEF (35±14% versus 30±12%; $P=0.032$) and more severely impaired circumferential and radial strains (GCS, -9.7±4.4% versus -7.9±3.5%; $P=0.045$; GRS, 13.3±7.7% versus 10.7±5.2%; $P=0.023$). SSRs and DSRs were more impaired in patients with septal LGE than in patients with non-septal LGE. However, GLS, SSR_L, and DSR_L were not associated with septal LGE (Table S1). Figure 3 shows a patient with septal midmyocardial LGE with impaired GCS and GRS but relatively preserved GLS. Comparisons between patients with (n=48) and without free-wall LGE (n=191) showed that LVEF and global strain (GCS, GLS, GRS), SSR, and DSR were also similar. Only the basal circumferential rotation was lower in patients with LGE involving the LV free wall (Table S2).

In the LGE-positive group, LGE was observed only in the septum or LV free wall in 28 (12%) patients and 32 (13%) patients, respectively. When comparing the two groups, patients with septal-only LGE had lower LVEF and more depressed GCS, GLS, GRS, SSRs, and DSRs (Table 3). Importantly, LGE was predominantly located in the basal segments in both groups, and the extent of fibrosis did not differ between groups.

Twist and Torsion

Basal and apical circumferential rotation, twist, twist per LV length, and torsion were similar in patients with and without LGE (Table 2). The apical rotation was reversed in 29% of the LGE--negative group and in 32% of the LGE-positive group, while basal rotation was detected in the counterclockwise rotation in 19% of the LGE-negative and in 21% of the LGE-positive group. Figure 4 shows representative examples of basal and apical systolic rotations (magnitude) in 3 patients with different LGE patterns. The apical rotation was reversed in 56% (33/56) of patients in the LBBB-positive group and in only 22% (40/183) of patients without LBBB; therefore, apical circumferential rotation was more impaired in patients with LBBB (net counterclockwise rotation, 0.8±1.1 versus 2.4±1.8; $P < 0.001$; magnitude, -0.9±2.7 versus 2.0±2.5; $P < 0.001$). On the contrary, basal rotation was reversed in 9% (5/56) of patients in the LBBB-positive group and in 24% (43/183) of patients in the LBBB-negative group. Basal circumferential rotation was less impaired in LBBB-positive group (net clockwise, -2.2±1.2 versus

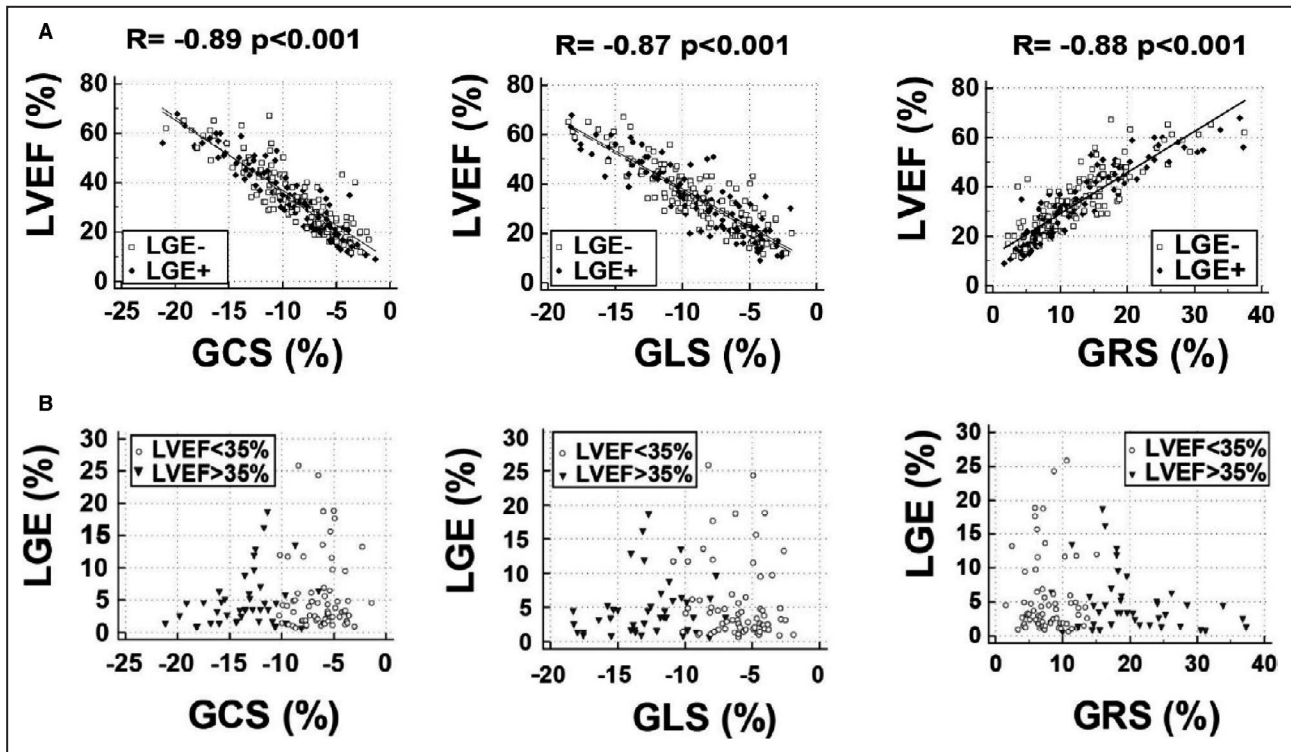


Figure 1. The associations of global strain values with left ventricular function and fibrosis.

A, Global strain values correlate with left ventricular ejection fraction. Left ventricular global strain values (circumferential [GCS], longitudinal [GLS], and radial [GRS]) correlated with left ventricular ejection fraction (LVEF) in the whole cohort and patients with (black rhombus) and without (empty square) late gadolinium enhancement (LGE) separately. **B**, Global strain values are not associated with late gadolinium enhancement (LGE). In patients with LGE ($n=109$), the extent of fibrosis (LGE%) did not correlate with global strain values in patients with moderately (LVEF >35%) (black triangle) or highly impaired (LVEF <35%) (empty circle) LV function.

-1.3 ± 1.09 ; $P=0.040$; magnitude, -2.0 ± 1.4 versus -1.0 ± 1.5 ; $P < 0.001$). LV twist (1.3 ± 2.1 versus 3.3 ± 2.6 ; $P < 0.0001$) and LV torsion (1.0 ± 0.8 versus 1.5 ± 1.1 ; $P=0.002$) were more impaired in patients with LBBB (Table S3).

When comparing isolated septal LGE and isolated free-wall LGE groups with similar degrees of fibrosis (LGE%, 4.4 [IQR, $3.0-5.8$] versus 5.1 [IQR, $3.4-6.9$]; $P=0.540$), torsional parameters were found to be similar (Table 3). Extent of fibrosis did not correlate with twist or torsion in the whole LGE=positive group, but did correlate in patients with LVEF >35%; LGE% correlated with the magnitude of apical systolic rotation ($r=0.36$; $P=0.018$), twist ($r=0.38$; $P=0.012$) and torsion ($r=0.39$; $P=0.010$).

Reproducibility of CMR Feature Tracking Parameters

Excellent intra- and interobserver reproducibility was observed for global strain values (GCS, GLS, and GRS) (Table 4). SSR had good reproducibility, while DSR values were less reproducible. The net basal and apical rotation (rotation in the anticipated direction) had higher intraclass correlation coefficient values compared with

the magnitude of rotation (maximum rotation regardless of direction) (Table 4). Twist, twist per length, and torsion demonstrated good intra- and interobserver reproducibility.

DISCUSSION

In this retrospective study of 239 patients with NICM, we found that CMR feature tracking-derived LV mechanical parameters of global strain (GCS, GLS, GRS), SSR (SSR_C, SSR_L, SSR_R), DSR (DSR_C, DSR_L, DSR_R), twist, and torsion were all impaired regardless of presence or absence of LGE. LV mechanical deformation parameters did not significantly correlate with extent of focal myocardial fibrosis. Patients with septal LGE had lower LVEF coupled with decreased GCS and GRS compared with patients without septal fibrosis. However, GLS was similar in both groups. In patients with similar extents of LV fibrosis, the septal location of LGE was associated with more depressed LV systolic function, including lower LVEF, global strains, SSRs, and DSRs compared with patients wherein LGE was limited to the LV free wall.

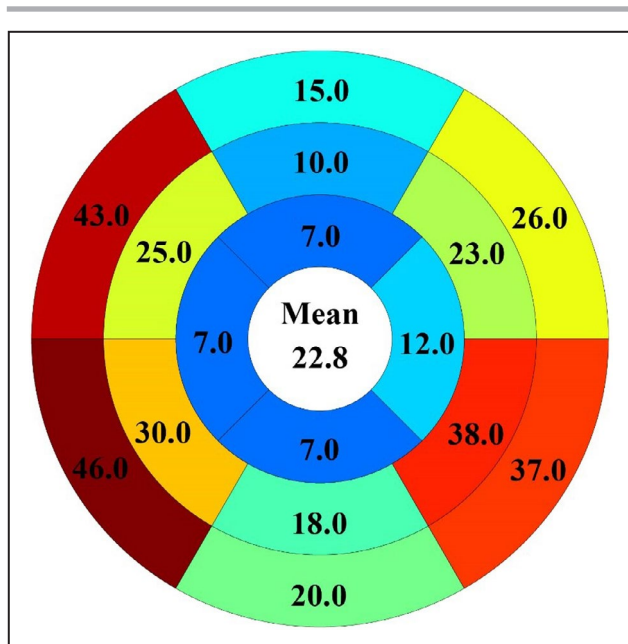


Figure 2. The distribution of LGE in all patients with fibrosis (n=109). The most frequent location of LGE was the basal septum (43% [n=40] and 46% [n=42]), followed by the basal (37% [n=34]) and mid inferolateral segments (38% [n=35]).

LV Mechanics in NICM

CMR feature tracking can assess cardiac performance in a wide variety of cardiac pathologies. The technique can be applied to quantification of LV and RV strain values, DSRs and SSRs, and LV myocardial torsion. Previous studies reporting data on healthy subjects showed that CMR feature tracking-derived GLS, GCS, and GRS values were not associated with age or sex.²⁶ The observed global LV mechanical parameters were lower in our NICM cohort than in healthy subjects.^{5,17,26,27} In this study, we quantified GLS, SSR_L, and DSR_L as the sum of the three long-axis apical views. GLS did not differentiate between patients with and without LGE in both the whole group and among patients with LVEF >35%. GLS, SSR_L, and DSR_L were not different in patients with or without septal LGE. GCS and GLS are major contributors to LV stroke volume and LVEF, but data describing the relative contributions of circumferential and longitudinal shortening are controversial.^{28–30} Previously, longitudinal shortening was believed to be the main driver of LVEF.^{29,30} However, an increasing number of studies report that midwall circumferential shortening has greater impact on LVEF than longitudinal shortening and can contribute as much as two-thirds of the stroke volume.^{31,32} In NICM, the LGE located in the midmyocardial wall affects myocardial fibers responsible for circumferential shortening of the LV. We found that the septal location of

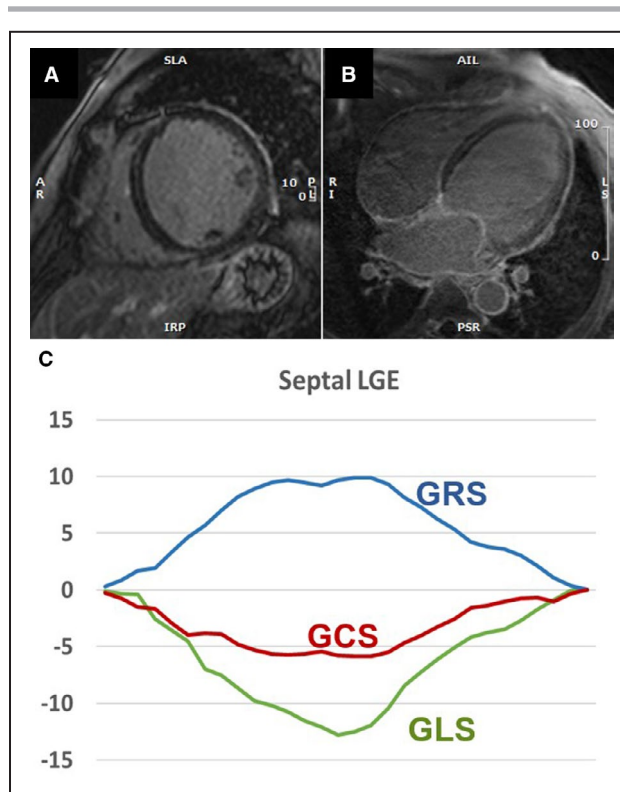


Figure 3. Patient with septal midmyocardial late gadolinium enhancement with impaired circumferential and radial shortening. Patient with septal late gadolinium enhancement (LGE) on short-axis (A) and long axis (B) LGE images. Patient has low left ventricular ejection fraction (LVEF=34%) with impaired global circumferential (GCS) and radial (GRS) strains but relatively less impaired longitudinal (GLS) strain values (C), suggesting that the impaired circumferential movement is associated with decreased LVEF.

LGE was associated with circumferential and radial shortening, but not with longitudinal shortening.

In the vast majority of prior CMR feature tracking studies, GCS and GRS are measured on a single short-axis slice or in 3 short-axis slices.^{8,18,26} In the current study, global strain values were calculated as the average of the mean curves of all LV segments on short-axis slices for comprehensive assessment of all LV mechanical parameters accounting for LGE location and whole heart LV remodeling. Excellent/good inter- and intraobserver reproducibility were detected for circumferential and radial mechanical values, and intraclass correlation coefficient values of GLS and GRS were comparable with previously published data in patients with NICM.³³

Previous studies show that presence of LBBB in NICM patients is related to impaired LV mechanics with reduction of LV twist.^{34,35} In agreement, we found that LBBB and consequential cardiac dyssynchrony is associated with reverse basal circumferential rotation and reduction of LV torsion and twist. Our study is the first to investigate the relation between presence of LBBB and

Table 3. Left Ventricular Parameters of Patients With Isolated Free-Wall Versus Isolated Septal Fibrosis

| Variables | Only Free-Wall LGE N=28 | Only Septal LGE N=32 | P Value |
|---------------------------|----------------------------|-------------------------|---------|
| LVEF, % | 38±16 | 30±12 | 0.026* |
| LVEDVi, mL/m ² | 125±40 | 144±34 | 0.056 |
| LVESVi, mL/m ² | 82±46 | 103±38 | 0.048* |
| LVSVi, mL/m ² | 44±14 | 40±13 | 0.336 |
| LVMi, g/m ² | 73±20 | 75±17 | 0.694 |
| GCS, % | -10.1±5.1 | -7.6±3.0 | 0.004* |
| SSR _C (1/s) | -0.61±0.21 | -0.45±0.18 | 0.003* |
| DSR _C (1/s) | 0.54±0.20 | 0.40±0.20 | 0.011* |
| GLS, % | -10.2±4.6 | -7.4±2.9 | 0.044* |
| SSR _L (1/s) | -10.1±5.1 | -7.6±3.0 | 0.003* |
| DSR _L (1/s) | 16.2±9.8 | 10.0±4.6 | 0.002* |
| GRS, % | 16.2±9.8 | 10.0±4.6 | 0.002* |
| SSR _R (1/s) | 0.85±0.38 | 0.59±0.29 | 0.004* |
| DSR _R (1/s) | -0.78±0.43 | -0.54±0.31 | 0.018* |
| Basal systolic rotation | | | |
| Net clockwise, ° | -1.22±1.2 | -1.60±-0.38 | 0.186 |
| Magnitude, ° | -0.83±1.65 | -1.45±1.26 | 0.110 |
| Apical systolic rotation | | | |
| Net counterclockwise, ° | 3.12±2.42 | 2.19±1.87 | 0.099 |
| Magnitude, ° | 2.56±3.29 | 1.45±2.89 | 0.171 |
| Twist, ° | 3.39±3.36 | 2.89±2.50 | 0.516 |
| Twist per length, °/cm | 0.48±0.47 | 0.43±0.37 | 0.645 |
| Torsion, °s ⁻¹ | 1.41±1.39 | 1.41±0.91 | 0.989 |
| LGE, g | 4.1 (3.0–5.6) | 6.0 (3.6–7) | 0.367 |
| LGE% | 4.4 (3.0–5.8) | 5.1 (3.4–6.9) | 0.540 |

DSR_C indicates circumferential diastolic strain rate; DSR_L, longitudinal diastolic strain rate; DSR_R, radial diastolic strain rate; GCS, global circumferential strain; GLS, global longitudinal strain; GRS, global radial strain; LGE, late gadolinium enhancement; LVEDVi, left ventricular end-diastolic volume index; LVESVi, left ventricular end-systolic volume index; LVEF, left ventricular ejection fraction; LVMi, left ventricular mass index; LVSVi, left ventricular stroke volume index; SSR_C, circumferential systolic strain rate; SSR_L, longitudinal systolic strain rate; and SSR_R, radial systolic strain rate.

*Significant value ($P < 0.05$).

impaired LV torsional parameters using CMR feature tracking in a large group of patients with NICM.

Nonischemic LV Fibrosis

Myocardial fibrosis is a common histopathologic finding in patients with NICM caused by an elevated amount of collagen and extracellular matrix proteins produced by activated fibroblasts.^{36,37} Myocardial fibrosis is the main contributor of the complex structural and functional cardiac abnormalities observed in patients with NICM, and the pattern of myocardial fibrosis can be identified with LGE imaging. Comparison of LGE extent across CMR studies can be challenging because of the wide variety of quantification techniques. Our

data support heterogeneity of nonischemic fibrosis in NICM, as the majority of LGE-positive cases (70%) had LGE detected in >1 LV segment (median number of LGE-positive segments is 3). LGE was most commonly identified in the basal (43%–46%) and mid (25%–30%) antero- and inferoseptal segments, while the second-most-common LGE location was the inferolateral wall (37%–38%). Literature data show that LGE data assessed by the 3 SD method may be suggestive of more diffuse processes or “micro-scarring.”³⁸ We performed LGE quantification using both 5 SD and 3 SD methods. Using 3 SD quantification in the LGE-positive group, the median amount of fibrosis was 11.0 g (IQR, 7.9–14.0) and the median LGE% was 7.5% (IQR, 6.0–9.0). The results of 5 SD and 3 SD LGE data were similar, and no correlation was found between 3 SD LGE% and LV function nor between 3 SD LGE% and different mechanical parameters. Finally, we decided to report the 5 SD data to make a more direct comparison with literature data reporting larger sample sizes.^{3,4,7}

LV Mechanics and Focal Fibrosis

Previous CMR feature tracking studies reported that CMR feature tracking derived mechanical parameters are useful to detect ischemic scar.^{12–14,39,40} However, limited studies are available reporting associations between LV mechanics and structural remodeling in patients with NICM.^{8,41,42} Taylor et al⁸ reported that the commonly observed septal midmyocardial LGE in NICM is associated with depressed GCS, twist, and torsion. In our study, septal LGE was also associated with impaired GCS and GRS, but not with torsion or twist. Patients with NICM with relatively preserved LVEF (>35%) is a significant burden in terms of prevalence, cardiovascular morbidity, and mortality. Based on our findings, LGE% did not correlate with global strain values (GCS, GLS, GRS) in this group; however, LGE% did correlate with the magnitude of apical systolic rotation and torsional parameters. These results may suggest that instead of global strain and strain rates, regional LV mechanical parameters could help better characterize the subgroup of patients with NICM with relatively preserved LV function. Further studies are needed to evaluate the role of regional strain values and torsional parameters in the prediction of outcomes in this subgroup of patients with preserved LV function. The correlation between LV fibrosis/scar and LV mechanics is influenced by multiple factors. Regardless of the amount or characteristics of the scar, LV wall thickness and global LV shape may also be important factors when studying the effect of scarring on LV mechanics. In HCM, for example, although LGE also has a nonischemic pattern, fibrosis in the hypertrophied segments (with

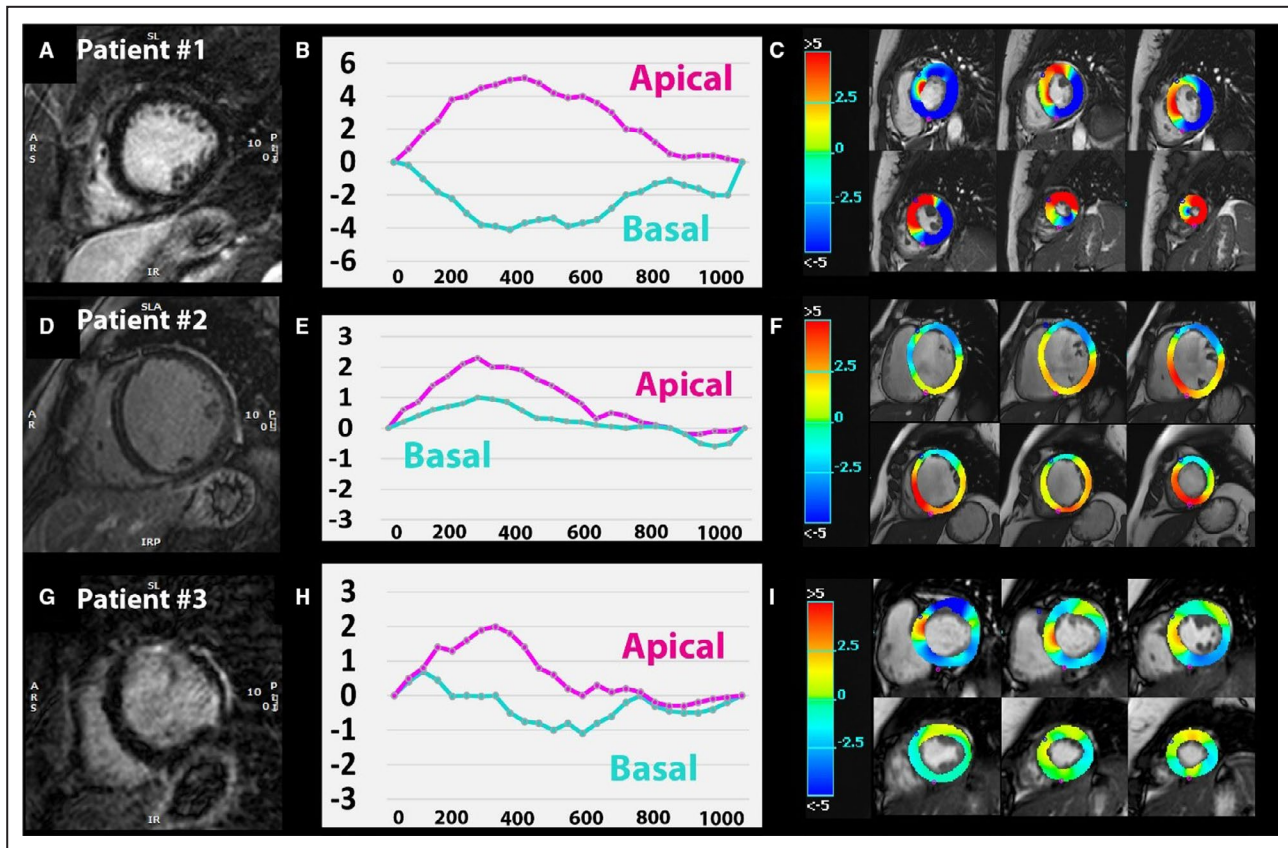


Figure 4. The location of LGE impacts LV mechanics.

Representative late gadolinium enhancement (LGE) images in 3 patients (first column **A**, **D**, and **G**), basal and apical circumferential rotation curves over time (second column **B**, **E**, and **H**), and circumferential rotation displayed as color-coded parametric maps (third column **C**, **F**, and **I**). Patient 1 without LGE (**A**) with physiologic clockwise basal rotation (negative curve [**B**] and blue basal slices on circumferential displacement map [**C**]) and counterclockwise apical rotation (positive curve on [**B**] and red apical slices on [**C**]). In patient 2, midmyocardial septal fibrosis (**D**) and reversed basal rotation (positive curve on **E**) were detected with dominant counterclockwise motion on the color-map (**F**). Patient 3 has free-wall LGE (**G**) and shows impaired basal rotation (partly positive basal curve on [**H**] and light blue/green colors on [**I**]).

disorganized myofibers) may have a different effect on LV mechanics compared with NICM, wherein LGE is located in the normal/thin wall of a dilated LV.

In the previously mentioned multicenter CMR feature tracking study,⁷ higher extents of LGE were found in subgroups with more depressed GLS, although patients with more impaired strain had predominantly ischemic etiology.⁷ In our study, strain values were generally impaired regardless of presence or absence of LGE. This observation remained when we compared patients who were LGE positive and patients who were LGE negative with an LVEF >35%. The extent of LGE did not correlate with LV mechanical parameters. However, the location of fibrosis affected LV mechanics. Patients with septal fibrosis had lower LVEF and impaired GCS and GRS strain values compared with patients without septal LGE. Longitudinal shortening was relatively preserved, supporting the notion that impaired circumferential movement is responsible for the impaired pump function.

LGE in the LV free wall did not affect global LV function, but was associated with impaired basal circumferential rotation and compensatory “hyperdynamic” apical rotation. As a result, twisting and torsion were not different between patients with or without free-wall LGE. Our results suggest that regional fibrosis may influence regional circumferential displacement without changing the global twisting motion.

Halliday et al⁴ reported that the presence of septal LGE is associated with a large increase in the risk of cardiac mortality and sudden cardiac death. They also showed that a risk assessment model including the presence and location of LGE was superior to models based on LGE extent and pattern. In our study, patients with septal LGE had lower LVEF and impaired GCS and GRS but preserved GLS. Furthermore, septal-only LGE was associated with depressed global strains and strain rates (SSR, DSR) compared with LGE involving the LV free wall. Our data support that the location of LGE is an important determinant of LV

Table 4. Inter- and Intraobserver Reproducibility of Left Ventricular Mechanical Parameters

| Variables | ICC of Intraobserver N=40 | ICC of Interobserver N=40 |
|---------------------------|---------------------------|---------------------------|
| GCS (%) | 0.99 (0.98–0.99) | 0.97 (0.96–0.99) |
| SSR _C (1/s) | 0.98 (0.97–0.99) | 0.94 (0.90–0.97) |
| DSR _C (1/s) | 0.97 (0.95–0.99) | 0.94 (0.89–0.97) |
| GLS (%) | 0.97 (0.96–0.99) | 0.94 (0.89–0.97) |
| SSR _L (1/s) | 0.89 (0.80–0.94) | 0.83 (0.70–0.91) |
| DSR _L (1/s) | 0.79 (0.63–0.88) | 0.68 (0.47–0.81) |
| GRS (%) | 0.99 (0.98–0.99) | 0.97 (0.96–0.99) |
| SSR _R (1/s) | 0.97 (0.96–0.99) | 0.90 (0.82–0.95) |
| DSR _R (1/s) | 0.75 (0.58–0.86) | 0.73 (0.54–0.84) |
| Basal rotation | | |
| Net clockwise, ° | 0.81 (0.64–0.90) | 0.75 (0.58–0.86) |
| Magnitude, ° | 0.74 (0.50–0.86) | 0.68 (0.40–0.83) |
| Apical rotation | | |
| Net counterclockwise, ° | 0.93 (0.86–0.96) | 0.88 (0.78–0.88) |
| Magnitude, ° | 0.90 (0.83–0.95) | 0.86 (0.73–0.92) |
| Twist, ° | 0.88 (0.78–0.93) | 0.72 (0.53–0.84) |
| Twist per length, %/cm | 0.82 (0.69–0.90) | 0.77 (0.61–0.87) |
| Torsion, °s ⁻¹ | 0.81 (0.67–0.89) | 0.76 (0.54–0.87) |

DSR_C, circumferential diastolic strain rate; DSR_L, longitudinal diastolic strain rate; DSR_R, radial diastolic strain rate; GCS, global circumferential strain; GLS, global longitudinal strain; GRS, global radial strain; ICC, intraclass correlation coefficient; SSR_C, circumferential systolic strain rate; SSR_L, longitudinal systolic strain rate; and SSR_R, radial systolic strain rate.

mechanics, while the extent of LGE does not correlate with mechanical parameters.

Limitations

Our study has several limitations. This is a single-center retrospective study of patients who were referred for a clinical CMR. Our cohort was mainly White and men, which is not necessarily representative of all patients with NICM. Since LGE located at the RV insertion points has uncertain clinical and prognostic significance,^{43–45} categorization of these patients as LGE positive or LGE negative is variable in the literature.^{3,4,8} In this study, patients with LGE limited to the RV anterior or inferior insertion zones (n=23) were categorized as LGE positive but were excluded from the subgroup of patients who were LGE positive with septal wall fibrosis. In this study, the vast majority of patients who were LGE positive had LGE% ≤5% (n=74), in whom more extensive fibrosis of the LV wall (especially LGE% >10%) might impact global LV mechanical parameters. Importantly, the LGE quantities of small/moderate extent and the LGE distribution in our cohort is consistent with previously reported data.^{3,4,44} T1 mapping is an emerging CMR technique that can identify diffuse myocardial fibrosis in a wide variety of clinical settings including NICM. In this study,

T1 maps are not available. Diffuse fibrosis may therefore be underestimated, which is one of the major limitations of the study.

CONCLUSIONS

In patients with NICM, LV mechanical parameters are universally impaired. The presence of LGE is not associated with impaired global strain (GCS, GLS, GRS), strain rate (SSR_C, SSR_L, SSR_R, DSR_C, DSR_L, DSR_R), or LV twisting motion. However, if extent of LGE is the same, the septal location of LGE is associated with more profound LV systolic dysfunction, impaired strain, and strain rate compared with LGE involving the LV free wall.

ARTICLE INFORMATION

Received April 17, 2020; accepted August 26, 2020.

Affiliations

From the Department of Medicine, Beth Israel Deaconess Medical Center, Harvard Medical School, Boston, MA.

Sources of Funding

Dr Nezafat receives grant funding by the National Institutes of Health 1R01HL129185-01, 1R01HL129157, 1R01HL127015, and R01HL15474401 (Bethesda, MD); and the American Heart Association 15EIA22710040 (Waltham, MA).

Disclosures

None.

Supplementary Materials

Tables S1–S3

REFERENCES

- Bozkurt B, Colvin M, Cook J, Cooper LT, Deswal A, Fonarow GC, Francis GS, Lenihan D, Lewis EF, McNamara DM, et al. Current diagnostic and treatment strategies for specific dilated cardiomyopathies: a scientific statement from the American Heart Association. *Circulation*. 2016;134:e579–e646.
- Japp AG, Gulati A, Cook SA, Cowie MR, Prasad SK. The diagnosis and evaluation of dilated cardiomyopathy. *J Am Coll Cardiol*. 2016;67:2996–3010.
- Becker MA, Cornel JH, Van de Ven PM, van Rossum AC, Allaart CP, Germans T. The prognostic value of late gadolinium-enhanced cardiac magnetic resonance imaging in nonischemic dilated cardiomyopathy: a review and meta-analysis. *JACC Cardiovasc Imaging*. 2018;11:1274–1284.
- Halliday BP, Baksi AJ, Gulati A, Ali A, Newsome S, Izgi C, Arzanauskaitė M, Lota A, Tayal U, Vassilio SV, et al. Outcome in dilated cardiomyopathy related to the extent, location, and pattern of late gadolinium enhancement. *JACC Cardiovasc Imaging*. 2019;12:1645–1655.
- Andre F, Steen H, Matheis P, Westkott M, Breuninger K, Sander Y, Kammerer R, Galuschky C, Giannitsis E, Korosoglou G, et al. Age- and gender-related normal left ventricular deformation assessed by cardiovascular magnetic resonance feature tracking. *J Cardiovasc Magn Reson*. 2015;17:25.
- Schuster A, Hor KN, Kowallick JT, Beerbaum P, Kutty S. Cardiovascular magnetic resonance myocardial feature tracking: concepts and clinical applications. *Circ Cardiovasc Imaging*. 2016;9:e004077. DOI: 10.1161/CIRCIMAGING.115.004077.
- Romano S, Judd RM, Kim RJ, Kim HW, Klem I, Heitner JF, Shah DJ, Jue J, White BE, Indorkar R, et al. Feature-tracking global longitudinal strain predicts death in a multicenter population of patients with ischemic and nonischemic dilated cardiomyopathy incremental to ejection

- fraction and late gadolinium enhancement. *JACC Cardiovasc Imaging*. 2018;11:1419–1429.
8. Taylor RJ, Umar F, Lin EL, Ahmed A, Moody WE, Mazur W, Stegemann B, Townend JN, Steeds RP, Leyva F. Mechanical effects of left ventricular midwall fibrosis in non-ischemic cardiomyopathy. *J Cardiovasc Magn Reson*. 2015;18:1.
 9. Buss SJ, Breuninger K, Lehrke S, Voss A, Galuschky C, Lossnitzer D, Andre F, Ehlermann P, Franke J, Taeger T, et al. Assessment of myocardial deformation with cardiac magnetic resonance strain imaging improves risk stratification in patients with dilated cardiomyopathy. *Eur Heart J Cardiovasc Imaging*. 2015;16:307–315.
 10. Breuninger K, Lehrke S, Matheis P, Sander Y, Kammerer R, Rust L, Galuschky C, Katus HA, Korosoglou G, Buss S. Feature tracking cardiac magnetic resonance imaging for the evaluation of myocardial strain in patients with dilated cardiomyopathy and in healthy controls. *J Cardiovasc Magn Reson*. 2013;15:P167.
 11. Sengupta PP, Tajik AJ, Chandrasekaran K, Khandheria BK. Twist mechanics of the left ventricle: principles and application. *JACC Cardiovasc Imaging*. 2008;1:366–376.
 12. Khan JN, Singh A, Nazir SA, Kanagala P, Gershlick AH, McCann GP. Comparison of cardiovascular magnetic resonance feature tracking and tagging for the assessment of left ventricular systolic strain in acute myocardial infarction. *Eur J Radiol*. 2015;84:840–848.
 13. Schuster A, Paul M, Bettencourt N, Morton G, Chiribiri A, Ishida M, Hussain S, Jogiya R, Kutty S, Bigalke B, et al. Cardiovascular magnetic resonance myocardial feature tracking for quantitative viability assessment in ischemic cardiomyopathy. *Int J Cardiol*. 2013;166:413–420.
 14. Mangion K, McComb C, Auger DA, Epstein FH, Berry C. Magnetic resonance imaging of myocardial strain after acute ST-segment-elevation myocardial infarction: a systematic review. *Circ Cardiovasc Imaging*. 2017;10:e006498. DOI: 10.1161/CIRCIMAGING.117.006498.
 15. Haland TF, Almaas VM, Hasselberg NE, Saberniak J, Leren IS, Hopp E, Edvardsen T, Haugaa KH. Strain echocardiography is related to fibrosis and ventricular arrhythmias in hypertrophic cardiomyopathy. *Eur Heart J Cardiovasc Imaging*. 2016;17:613–621.
 16. Neisius U, Myerson L, Fahmy AS, Nakamori S, El-Rewaify H, Joshi G, Duan C, Manning WJ, Nezafat R. Cardiovascular magnetic resonance feature tracking strain analysis for discrimination between hypertensive heart disease and hypertrophic cardiomyopathy. *PLoS One*. 2019;14:e0221061.
 17. Taylor RJ, Moody WE, Umar F, Edwards NC, Taylor TJ, Stegemann B, Townend JN, Hor KH, Steeds RP, Wojciech M, et al. Myocardial strain measurement with feature-tracking cardiovascular magnetic resonance: normal values. *Eur Heart J Cardiovasc Imaging*. 2015;16:871–881.
 18. Morton G, Schuster A, Jogiya R, Kutty S, Beerbaum P, Nagel E. Inter-study reproducibility of cardiovascular magnetic resonance myocardial feature tracking. *J Cardiovasc Magn Reson*. 2012;14:43.
 19. Young AA, Cowan BR. Evaluation of left ventricular torsion by cardiovascular magnetic resonance. *J Cardiovasc Magn Reson*. 2012;14:49.
 20. Rüssel IK, Tecelão SR, Kuijper JP, Heethaar RM, Marcus JT. Comparison of 2D and 3D calculation of left ventricular torsion as circumferential-longitudinal shear angle using cardiovascular magnetic resonance tagging. *J Cardiovasc Magn Reson*. 2009;11:8.
 21. Kowallick JT, Morton G, Lamata P, Jogiya R, Kutty S, Lotz J, Hasenfuß G, Nagel E, Chiribiri A, Schuster A. Inter-study reproducibility of left ventricular torsion and torsion rate quantification using MR myocardial feature tracking. *J Magn Reson Imaging*. 2016;43:128–137.
 22. Mikami Y, Cornhill A, Heydari B, Joncas SX, Almeahmadi F, Zahrani M, Bokhari M, Stirrat J, Yee R, Merchant N, et al. Objective criteria for septal fibrosis in non-ischemic dilated cardiomyopathy: validation for the prediction of future cardiovascular events. *J Cardiovasc Magn Reson*. 2017;18:82.
 23. Almeahmadi F, Joncas SX, Nevis I, Zahrani M, Bokhari M, Stirrat J, Fine NM, Yee R, White JA. Prevalence of myocardial fibrosis patterns in patients with systolic dysfunction: prognostic significance for the prediction of sudden cardiac arrest or appropriate implantable cardiac defibrillator therapy. *Circ Cardiovasc Imaging*. 2014;7:593–600.
 24. Neisius U, El-Rewaify H, Kucukseymen S, Tsao CW, Mancio J, Nakamori S, Manning WJ, Nezafat R. Texture signatures of native myocardial T1 as novel imaging markers for identification of hypertrophic cardiomyopathy patients without scar. *J Magn Reson Imaging*. 2020;52:906–919.
 25. Shrout PE, Fleiss JL. Intraclass correlations: uses in assessing rater reliability. *Psychol Bull*. 1979;86:420.
 26. Vo HQ, Marwick TH, Negishi K. MRI-derived myocardial strain measures in normal subjects. *JACC Cardiovasc Imaging*. 2018;11:196–205.
 27. Schuster A, Stahnke V-C, Unterberg-Buchwald C, Kowallick J, Lamata P, Steinmetz M, Kutty S, Fasshauer M, Staab W, Sohns JM, et al. Cardiovascular magnetic resonance feature-tracking assessment of myocardial mechanics: intervendor agreement and considerations regarding reproducibility. *Clin Radiol*. 2015;70:989–998.
 28. Wandt B, Brodin L-A, Lundbäck S. Misinterpretation about the contribution of the left ventricular long-axis shortening to the stroke volume. *Am J Physiol Heart Circ Physiol*. 2006;291:H2550.
 29. Carlsson M, Cain P, Holmqvist C, Stahlberg F, Lundback S, Arheden H. Total heart volume variation throughout the cardiac cycle in humans. *Am J Physiol Heart Circ Physiol*. 2004;287:H243–H250.
 30. Emilsson K, Brudin L, Wandt B. The mode of left ventricular pumping: is there an outer contour change in addition to the atrioventricular plane displacement? *Clin Physiol*. 2001;21:437–446.
 31. Stokke TM, Hasselberg NE, Smedsrud MK, Sarvari SI, Haugaa KH, Smiseth OA, Edvardsen T, Remme EW. Geometry as a confounder when assessing ventricular systolic function: comparison between ejection fraction and strain. *J Am Coll Cardiol*. 2017;70:942–954.
 32. MacIver DH. The relative impact of circumferential and longitudinal shortening on left ventricular ejection fraction and stroke volume. *Exp Clin Cardiol*. 2012;17:5.
 33. Pi S-H, Kim SM, Choi J-O, Kim EK, Chang S-A, Choe YH, Lee SC, Jeon ES. Prognostic value of myocardial strain and late gadolinium enhancement on cardiovascular magnetic resonance imaging in patients with idiopathic dilated cardiomyopathy with moderate to severely reduced ejection fraction. *J Cardiovasc Magn Reson*. 2018;20:36.
 34. Emara A, Badran HM, Abdou W, Fahim N, Fathi M, Yacoub MH. Impact of left bundle branch block on left ventricular mechanics in patients with idiopathic dilated cardiomyopathy. *World J Cardiovasc Dis*. 2019;9:132–148.
 35. Foell D, Jung BA, Germann E, Staehle F, Bode C, Hennig J, Markl M. Segmental myocardial velocities in dilated cardiomyopathy with and without left bundle branch block. *J Magn Reson Imaging*. 2013;37:119–126.
 36. Krenning G, Zeisberg EM, Kalluri R. The origin of fibroblasts and mechanism of cardiac fibrosis. *J Cell Physiol*. 2010;225:631–637.
 37. Kong P, Christia P, Frangogiannis NG. The pathogenesis of cardiac fibrosis. *Cell Mol Life Sci*. 2014;71:549–574.
 38. Treibel TA, López B, González A, Menacho K, Schofield RS, Ravassa S, Fontana M, White SK, DiSalvo C, Roberts N, et al. Reappraising myocardial fibrosis in severe aortic stenosis: an invasive and non-invasive study in 133 patients. *Eur Heart J*. 2018;39:699–709.
 39. Maret E, Todt T, Brudin L, Nylander L, Swahn E, Ohlsson JL, Engvall JE. Functional measurements based on feature tracking of cine magnetic resonance images identify left ventricular segments with myocardial scar. *Cardiovasc Ultrasound*. 2009;7:53.
 40. Cameli M, Mondillo S, Righini FM, Lisi M, Dokollari A, Lindqvist P, Maccherini M, Henein M. Left ventricular deformation and myocardial fibrosis in patients with advanced heart failure requiring transplantation. *J Card Fail*. 2016;22:901–907.
 41. Mazurkiewicz Ł, Petryka J, Spiewak M, Miłosz-Wieczorek B, Werys K, Malek ŁA, Polanska-Skrzypczyk M, Ojrzynska N, Kubik A, Marczak M, et al. Biventricular mechanics in prediction of severe myocardial fibrosis in patients with dilated cardiomyopathy: CMR study. *Eur J Radiol*. 2017;91:71–81.
 42. Nanjo S, Yoshikawa K, Harada M, Inoue Y, Namiki A, Nakano H, Yamazaki J. Correlation between left ventricular diastolic function and ejection fraction in dilated cardiomyopathy using magnetic resonance imaging with late gadolinium enhancement. *Circ J*. 2009;73:1939–1944.
 43. Gaztanaga J, Paruchuri V, Elias E, Wilner J, Islam S, Sawit S, Viles-Gonzalez J, Sanz J, Garcia MJ. Prognostic value of late gadolinium enhancement in nonischemic cardiomyopathy. *Am J Cardiol*. 2016;118:1063–1068.
 44. Neilan TG, Coelho-Filho OR, Danik SB, Shah RV, Dodson JA, Verdini DJ, Tokuda M, Daly CA, Tedrow UB, Stevenson WG, et al. CMR quantification of myocardial scar provides additive prognostic information in non-ischemic cardiomyopathy. *JACC Cardiovasc Imaging*. 2013;6:944–954.
 45. Yi J-E, Park J, Lee H-J, Shin DG, Kim Y, Kim M, Kwon K, Pyun WB, Kim YJ, Joung B. Prognostic implications of late gadolinium enhancement at the right ventricular insertion point in patients with non-ischemic dilated cardiomyopathy: a multicenter retrospective cohort study. *PLoS One*. 2018;13:e0208100.

Supplemental Material

Table S1. Cardiac magnetic resonance left and right ventricular mechanical parameters in non-ischemic cardiomyopathy patients with and without septal fibrosis.

| Variables | No septal LGE | Septal LGE | P value |
|-----------------------------|---------------|--------------|---------|
| | N = 187 | N = 52 | |
| LVEDVi (ml/m ²) | 130 ± 36 | 140 ± 35 | 0.236 |
| LVESVi (ml/m ²) | 88 ± 40 | 101 ± 40 | 0.046* |
| LVSVi (ml/m ²) | 42 ± 12 | 39 ± 12 | 0.175 |
| LVEF (%) | 35 ± 14 | 30 ± 12 | 0.032* |
| LVMi (g/m ²) | 71 ± 21 | 74 ± 18 | 0.317 |
| RVEDVi (ml/m ²) | 91 ± 25 | 89 ± 25 | 0.594 |
| RVESVi (ml/m ²) | 50 ± 28 | 52 ± 27 | 0.724 |
| RVSVi (ml/m ²) | 42 ± 11 | 37 ± 11 | 0.026* |
| RVEF (%) | 46 ± 14 | 44 ± 15 | 0.436 |
| RVEF/LVEF | 1.4 ± 0.4 | 1.6 ± 0.5 | 0.023* |
| RVEDV/LVEDV | 0.73 ± 0.20 | 0.66 ± 0.18 | 0.039* |
| GCS (%) | -9.7 ± 4.4 | -7.9 ± 3.5 | 0.045* |
| SSR _C (1/s) | -0.54 ± 0.22 | -0.44 ± 0.22 | 0.007* |
| DSR _C (1/s) | 0.52 ± 0.26 | 0.41 ± 0.18 | 0.042* |
| GLS (%) | -8.9 ± 4.2 | -8.0 ± 3.5 | 0.161 |
| SSR _L (1/s) | -5.00 ± 0.21 | -0.45 ± 0.21 | 0.143 |
| DSR _L (1/s) | 0.48 ± 0.19 | 0.44 ± 0.18 | 0.178 |
| GRS (%) | 13.3 ± 7.7 | 10.7 ± 5.2 | 0.023* |
| SSR _R (1/s) | 0.71 ± 0.35 | 0.59 ± 0.29 | 0.022* |
| DSR _R (1/s) | -0.69 ± 0.46 | -0.55 ± 0.28 | 0.045* |

Basal systolic rotation

| | | | |
|-------------------|------------|------------|-------|
| Net Clockwise (°) | -1.5 ± 1.1 | -1.4 ± 1.1 | 0.653 |
| Magnitude (°) | -1.3 ± 1.5 | -1.2 ± 1.5 | 0.682 |

Apical systolic rotation

| | | | |
|-----------------------------|-------------|-------------|-------|
| Net Counterclockwise (°) | 2.1 ± 1.8 | 1.9 ± 1.7 | 0.756 |
| Magnitude (°) | 1.4 ± 2.8 | 1.1 ± 2.8 | 0.593 |
| Twist (°) | 2.7 ± 2.6 | 2.3 ± 2.7 | 0.423 |
| Twist per length (°/cm) | 0.39 ± 0.39 | 0.35 ± 0.43 | 0.504 |
| Torsion (°s ⁻¹) | 1.23 ± 1.08 | 1.19 ± 1.21 | 0.856 |

DSR_C= circumferential diastolic strain rate; DSR_L= longitudinal diastolic strain rate; DSR_R= radial diastolic strain rate; GCS= global circumferential strain; GLS= global longitudinal strain; GRS= global radial strain; LGE= late-gadolinium enhancement; LVEDVi= left ventricular end-diastolic volume index; LVESVi= left ventricular end-systolic volume index; LVEF=left ventricular ejection fraction; LVMi= left ventricular mass index; LVSVi= left ventricular stroke volume index; RVEDV= right ventricular end-diastolic volume; RVEDVi= right ventricular end-diastolic volume index; RVESVi= left ventricular end-systolic volume index; RVEF= right ventricular ejection fraction; RVSVi= right ventricular stroke volume index; SSR_C= circumferential systolic strain rate; SSR_L= longitudinal systolic strain rate; SSR_R= radial systolic strain rate; *Significant value (P < 0.05)

Table S2. Cardiac magnetic resonance left ventricular mechanical parameters in non-ischemic cardiomyopathy patients with and without free wall fibrosis.

| Variables | No free wall LGE | Free wall LGE | P value |
|-----------------------------|------------------|---------------|---------|
| | N = 191 | N = 48 | |
| LVEDVi (ml/m ²) | 133 ± 35 | 128 ± 39 | 0.397 |
| LVESVi (ml/m ²) | 91 ± 38 | 88 ± 45 | 0.540 |
| LVSVi (ml/m ²) | 41 ± 12 | 41 ± 12 | 0.898 |
| LVEF (%) | 34 ± 14 | 35 ± 15 | 0.473 |
| LVMi (g/m ²) | 72 ± 20 | 73 ± 20 | 0.599 |
| GCS (%) | -8.9 ± 4.0 | -9.9 ± 4.7 | 0.102 |
| SSR _C (1/s) | -0.51 ± 0.22 | -0.54 ± 0.26 | 0.377 |
| DSR _C (1/s) | 0.50 ± 0.26 | 0.50 ± 0.19 | 0.923 |
| GLS (%) | -8.5 ± 3.4 | -9.7 ± 4.5 | 0.058 |
| SSR _L (1/s) | -0.48 ± 0.20 | -0.52 ± 0.21 | 0.291 |
| DSR _L (1/s) | 0.47 ± 0.19 | 0.48 ± 0.16 | 0.751 |
| GRS (%) | 12.4 ± 6.9 | 14.4 ± 8.7 | 0.085 |
| SSR _R (1/s) | 0.67 ± 0.34 | 0.77 ± 0.36 | 0.096 |
| DSR _R (1/s) | -0.65 ± 0.44 | -0.7 ± 0.39 | 0.45 |
| Basal systolic rotation | | | |
| Net Clockwise (°) | -1.6 ± 1.1 | -1.1 ± 1.2 | 0.032* |
| Magnitude (°) | -1.4 ± 1.4 | -0.7 ± 1.7 | 0.008* |
| Apical systolic rotation | | | |
| Net Counterclockwise (°) | 1.9 ± 1.7 | 2.6 ± 2.2 | 0.033* |
| Magnitude (°) | 1.1 ± 2.7 | 1.9 ± 3.2 | 0.141 |

| | | | |
|-----------------------------|-------------|-------------|-------|
| Twist (°) | 2.6 ± 2.4 | 2.6 ± 3.4 | 0.954 |
| Twist per length (°/cm) | 0.38 ± 0.37 | 0.38 ± 0.51 | 0.951 |
| Torsion (°s ⁻¹) | 1.23 ± 1.00 | 1.17 ± 1.52 | 0.714 |

DSRc= circumferential diastolic strain rate; DSRL= longitudinal diastolic strain rate; DSRR= radial diastolic strain rate; GCS= global circumferential strain; GLS= global longitudinal strain; GRS= global radial strain; LGE= late-gadolinium enhancement; LVEDVi= left ventricular end-diastolic volume index; LVESVi= left ventricular end-systolic volume index; LVEF=left ventricular ejection fraction; LVMi= left ventricular mass index; LVSVi= left ventricular stroke volume index; SSRC= circumferential systolic strain rate; SSRL= longitudinal systolic strain rate; SSRR= radial systolic strain rate; *Significant value (P < 0.05)

Table S3. Cardiac magnetic resonance left ventricular mechanical parameters in non-ischemic cardiomyopathy patients with and without left bundle branch block (LBBB).

| | LBBB+ | LBBB- | |
|---------------------------------|---------------|----------------|----------------|
| Variables | N = 56 | N = 183 | P value |
| Basal systolic rotation | | | |
| Net Clockwise (°) | -2.2 ± 1.2 | -1.3 ± 1.1 | 0.040* |
| Magnitude (°) | -2.0 ± 1.4 | -1.0 ± 1.5 | 0.001* |
| Apical systolic rotation | | | |
| Net Counterclockwise (°) | 0.8 ± 1.1 | 2.4 ± 1.8 | 0.001* |
| Magnitude (°) | -0.9 ± 2.7 | 2.0 ± 2.5 | 0.001* |
| Twist (°) | 1.3 ± 2.1 | 3.3 ± 2.6 | 0.001* |
| Torsion (°s ⁻¹) | 1.0 ± 0.8 | 1.5 ± 1.1 | 0.002* |